Chinese Journal of
POLYMER SCIENCE

RESEARCH ARTICLE

https://doi.org/10.1007/s10118-022-2758-5
Chinese J. Polym. Sci. **2022**, *40*, 1369–1379

Highly Efficient and Thermal Robust Cobalt Complexes for 1,3-Butadiene Polymerization

Liang Fang[a], Wen-Peng Zhao[b], Chun-Yu Zhang[b], Xue-Quan Zhang[b], Xian-De Shen[a*], Heng Liu[b*], and Toyoji Kakuchi[a,c*]

[a] *Research Center for Polymer Materials, School of Materials Science and Engineering, Changchun University of Science and Technology, Jilin 130022, China*
[b] *Key Laboratory of Rubber-Plastics, Ministry of Education/Shandong Provincial Key Laboratory of Rubber-Plastics, Qingdao University of Science & Technology, Qingdao 266061, China*
[c] *Division of Applied Chemistry, Faculty of Engineering, Hokkaido University, Sapporo, Hokkaido 060-8628, Japan*

Electronic Supplementary Information

Abstract A family of highly bulky bis(salicylaldiminate) Co(II) complexes bearing cavity-like conformations are disclosed herein. Due to their unique bulky nature around the cobalt atoms that are reflected from space-filling models and the buried volume percentages, obviously longer bond distances of Co—N and Co—O are revealed from those complexes. Moreover, because of these well-protected active species, the cobalt complexes are able to catalyze 1,3-butadiene polymerization in high yields at extreme low catalyst concentrations, revealing a ultra high catalytic efficiency. At a ratio of 50000, all the complexes can afford polybutadiene with yields higher than 90%. Furthermore, the highly steric bulkiness of the ligand can also significantly enhance the thermostability of the active species. At temperature of 80–120 °C, the complexes are able to successfully maintain high activities, giving polymer yields up to 90%.

Keywords Butadiene polymerization; Bis(salicylaldiminate) Co(II) complexes; Ultra high catalytic efficiency

Citation: Fang, L.; Zhao, W. P.; Zhang, C. Y.; Zhang, X. Q.; Shen, X. D.; Liu, H.; Kakuchi, T. Highly efficient and thermal robust cobalt complexes for 1,3-butadiene polymerization. *Chinese J. Polym. Sci.* **2022**, *40*, 1369–1379.

INTRODUCTION

Late-transition metal is an indispensable block of the whole catalysts building. Thanks to their inherent low oxophilic nature, which brings good heteroatom tolerance ability and therefore a broader reaction substrate scope, multitudinous late-transition metal based precatalysts have been designed during the past century for promoting small molecule transformations, polymerizing C=C-containing monomers. Regarding the olefin/diene polymerization field, such a less oxophilic property become more meaningful because these precatalysts are capable of one-pot catalyzing olefin/diene monomer with polar comonomer to directly afford functional polymer products, which greatly outbalance traditional non-polar polymer counterparts in regard to compositing with inorganic fillers, affinity for dyes, adhesive properties, *etc.*, and has long been recognized as the "Holy Grail" for such a field.[1–25] Despite of these superiorities, late-transition metal based catalysts also suffered from some issues that are urgent to be addressed: (i) general lower catalytic efficiency due to lower electrophilicity and therefore lower monomer binding ability when comparing to the early-transition metals; (ii) relative lower molecular weight of the resultant polymers due to the greater tendency for β-H elimination; (3) poor thermostability of the active species. Designing effective catalyst that is able to conquer these three issues is highly desired for the polyolefin/polydienes industry.

Late transition metal mediated diene polymerizations is currently one of the widely used strategy to access commercial available polydiene synthetic rubbers.[26–39] Two representative systems are $CoCl_2$/donor/$AlEt_xCl_{3-x}$ and $Ni(OCOR)_2$/$BF_3{\cdot}OEt_2$/$AlEt_3$. Despite of their large-scale industrialization, their ill-defined nature of the corresponding active species prompts more scientists to design single-site precatalyst systems that demonstrate better controllability of the whole polymerization process. One prominent example is the imine-based cobalt(II) system. Due to the ease manipulation of imine structure, which allows facile fine-tuning the polymerization performances from steric and electronic aspects, diversified imine-based ligands, including bis(imino)pyridine,[31,40] α-diimine,[41] β-triketimine,[42] salicylaldimine,[43–47] pyridine-2-imine,[32,48] 1,10-phenanthroline-2-pyrazolyl,[49] bis(oxazolinyl)pyridine,[50,51] bis(imidazolyl)pyridine,[52,53] *etc.*, have been employed to support cobalt metal to regulate diene polymerization behaviors from molecular level. Nevertheless,

* Corresponding authors, E-mail: shenxiande@cust.edu.cn (X.D.S.)
E-mail: hengliu@qust.edu.cn (H.L.)
E-mail: kakuchi@eng.hokudai.ac.jp (T.K.)

Received March 3, 2022; Accepted April 9, 2022; Published online July 20, 2022

© Chinese Chemical Society
Institute of Chemistry, Chinese Academy of Sciences

these systems also more or less reveal the above-mentioned deficiencies. For some of them, comparatively higher precatalyst loading is required in order to achieve acceptable product yields, and for some ones, polymerizations are restricted to relative lower temperatures (20–50 °C) because high temperature imposes strong negative influence on the catalytic efficiency. In this contribution, we disclose a family of highly bulky bis(salicylaldiminate) Co(II) complexes that bear cavity-like conformations. Because of the unique location of the cobalt center in the cavity of the complexes, the formed active species could be well-protected from the impurities from the polymerization medium, and thereafter reveal ultra-high catalytic efficiency even at an extreme low precatalyst loading. Moreover, the being protected active species simultaneously reveals high thermal robust, which could afford very high polymer yields at high temperature up to 120 °C. These findings provide an effective strategy to enhance the overall catalytic performance of late-transition metal catalysts. Details discussion will be shown in the following.

EXPERIMENTAL

General Considerations

All manipulations of air and/or moisture sensitive compounds were carried out under a dry and oxygen-free argon atmosphere by using Schlenk techniques or under a nitrogen atmosphere in a glovebox. The solvents were refluxed over CaH_2 or sodium-benzophenone and distilled prior to use. 1,3-Butadiene was obtained from Lanzhou Petrochemical Company and purified by passing through four columns packed with 4 Å molecular sieves and KOH. Other chemicals were purchased commercially. ^{1}H-NMR (400 MHz) and ^{13}C-NMR (100 MHz) were recorded on a Varian Unity spectrometer in $CDCl_3$ at ambient temperature using tetramethylsilane as an internal standard. FTIR spectra were recorded using a BRUKER Vertex-70 FTIR spectrometer. Mass spectrograms of cobalt complexes were recorded using the Brooker IMPACT II TOF UHR-TOF ultra-high resolution ESI-Quadrupole Time-of-Flight mass spectrometry system The proportion of *cis*-1,4 and *trans*-1,4 units of the polymer was determined by FTIR spectra. The number-average molecular weights (M_n) and molecular weight distributions (M_w/M_n) of polymers were measured at 30 °C by gel permeation chromatography (GPC) equipped with a Waters 515 HPLC pump, four columns (HMW 7 THF, HMW 6E THF × 2, HMW 2THF), and a Waters 2414 refractive index detector. Tetrahydrofuran was used as the eluent at a flow rate of 1.0 mL·min^{-1} against polystyrene as the calibration.

Synthesis and Characterization of the Ligands and Complexes

L1. A mixture of 3,5-di-*tert*-butyl-2-hydroxybenzaldehyde (3.54 mmol, 0.83 g), 2,6-bis[bis(4-methoxyphenyl)methyl]-4-methyl benzenamine (3.54 mmol, 2.0 g) and a catalytic amount of *p*-toluenesulfonic acid (0.03 g) in 50 mL of ethanol was refluxed for 6 h and cooled down to room temperature. The resultant precipitate was filtered and dried in vacuo at 40 °C overnight, and light brown powder was obtained as the product. Yield 88.3%. ^{1}H-NMR (400 MHz, chloroform-d, *δ*, ppm): 12.99 (s, 1H), 7.35 (d, *J*=2.4 Hz, 1H), 6.99 (d, *J*=7.9 Hz, 2H), 6.92 (d, *J*=8.6 Hz, 8H), 6.75 (d, *J*=2.8 Hz, 4H), 6.68 (d, *J*=32.7 Hz, 6H), 6.24 (d, *J*=2.4 Hz, 1H), 5.35 (s, 2H), 3.75 (s, 12H), 2.17 (s, 3H), 1.46 (s, 9H), 1.23 (s, 9H). ^{13}C-NMR (101 MHz, chloroform-d, *δ*, ppm): 169.77, 158.17 (d, *J*=29.0 Hz), 157.97, 145.97, 139.86, 136.37 (d, *J*=18.4 Hz), 135.55, 133.35, 130.66, 128.73, 127.50, 126.91, 117.64, 113.97, 113.64, 55.28, 50.73, 35.15, 34.12, 31.55, 29.60, 21.59. ESI-MS (*m/z*): calcd. for $C_{52}H_{57}NO_5$: 775.42; Found 775.40[M]$^+$.

L2 was prepared in a similar method to **L1**. Yield 86.9%. ^{1}H-NMR (400 MHz, chloroform-d, *δ*, ppm): 12.67 (d, *J*=15.4 Hz, 1H), 7.38 (d, *J*=2.3 Hz, 1H), 6.99–6.94 (m, 7H), 6.94–6.89 (m, 7H), 6.87 (s, 3H), 6.60 (s, 2H), 6.21 (d, *J*=2.2 Hz, 1H), 5.40 (s, 2H), 2.18 (s, 3H), 1.45 (s, 9H), 1.24 (s, 9H). ^{13}C-NMR (101 MHz, chloroform-d, *δ*, ppm): 169.77, 158.17 (d, *J*=29.0 Hz), 157.97, 145.97, 139.86, 136.37 (d, *J*=18.4 Hz), 135.55, 133.35, 130.66, 128.73, 127.50, 126.91, 117.64, 113.97, 113.64, 55.28, 50.73, 35.15, 34.12, 31.55, 29.60, 21.59. ESI-MS (*m/z*): calcd. for $C_{48}H_{45}F_4NO$: 727.34; Found 727.30[M]$^+$.

L3 was prepared in a similar method to **L1**. Yield 83.4%. ^{1}H-NMR (400 MHz, chloroform-d, *δ*, ppm): 12.96 (d, *J*=3.5 Hz, 1H), 7.34 (d, *J*=2.4 Hz, 1H), 6.99 (d, *J*=7.9 Hz, 8H), 6.91 (t, *J*=7.1 Hz, 9H), 6.66 (s, 2H), 6.16 (d, *J*=2.4 Hz, 1H), 5.36 (s, 2H), 2.28 (s, 12H), 2.16 (s, 3H), 1.46 (s, 9H), 1.23 (s, 9H). ^{13}C-NMR (101 MHz, chloroform-d, *δ*, ppm): 169.93, 158.04, 146.11, 141.03, 139.71, 136.43, 135.55, 135.29, 133.29, 129.69, 129.36, 128.91 (d, *J*=14.3 Hz), 127.44, 126.94, 117.66, 51.64, 35.15, 34.09, 31.56, 29.59, 21.59, 21.15. ESI-MS (*m/z*): calcd. for $C_{52}H_{57}NO$: 711.44; Found 711.50 [M]$^+$.

L4 was prepared in a similar method to **L1**. Yield 77.9%. ^{1}H-NMR (400 MHz, chloroform-d, *δ*, ppm): 12.92 (d, *J*=7.3 Hz, 1H), 7.34 (d, *J*=2.1 Hz, 1H), 7.17 (d, *J*=14.1, 6.9 Hz, 1H), 6.98 (t, *J*=7.8 Hz, 8H), 6.93–6.86 (m, 9H), 6.17 (d, *J*=2.3 Hz, 1H), 5.38 (s, 2H), 3.72 (q, *J*=7.0 Hz, 2H), 2.28 (s, 10H), 1.45 (s, 9H), 1.25 (d, *J*=7.0 Hz, 3H), 1.23 (s, 9H), 1.09 (d, *J*=6.1 Hz, 9H). ^{13}C-NMR (101 MHz, chloroform-d, *δ*, ppm): 169.82, 158.03 (d, *J*=5.9 Hz), 146.41, 145.96, 141.19, 139.69, 136.46, 135.47, 134.67, 129.74 (d, *J*=17.7 Hz), 128.92, 128.28, 127.42, 126.93, 126.24, 125.27, 117.66 (d, *J*=7.3 Hz), 51.90, 35.17, 34.59, 34.10, 31.51 (d, *J*=11.6 Hz), 29.60, 21.15. ESI-MS (*m/z*): calcd. for $C_{55}H_{63}NO$: 753.49 Found 753.50 [M]$^+$.

L5 was prepared in a similar method to **L1**. Yield 85.2%. ^{1}H-NMR (400 MHz, chloroform-d, *δ*, ppm): 13.02 (s, 1H), 7.34 (d, *J*=2.0 Hz, 1H), 7.02–6.88 (m, 17H), 6.43 (s, 2H), 6.15 (d, *J*=2.1 Hz, 1H), 5.38 (s, 2H), 3.56 (s, 3H), 2.28 (s, 12H), 1.46 (s, 9H), 1.23 (s, 9H). ^{13}C-NMR (101 MHz, chloroform-d, *δ*, ppm): 170.25, 157.99, 155.92, 142.04, 140.67, 139.61, 136.77, 136.35, 135.58, 129.54, 128.93, 127.34, 126.82, 117.57, 113.82, 55.18, 51.73, 35.06, 34.00, 31.46, 29.49, 21.04. Found: C, 85.49 H, 7.60 N, 1.85 ESI-MS (*m/z*): calcd. for $C_{52}H_{57}NO_2$: 727.44; Found 727.40 [M]$^+$.

L6 was prepared in a similar method to **L1**. Yield 70.4%. ^{1}H-NMR (400 MHz, chloroform-d, *δ*, ppm): 12.96 (d, *J*=17.5 Hz, 1H), 7.34 (d, *J*=2.4 Hz, 1H), 7.24–7.11 (m, 12H), 7.07–7.00 (m, 8H), 6.43 (s, 2H), 5.48 (s, 2H), 3.55 (s, 3H), 1.46 (s, 9H), 1.22 (s, 9H). ^{13}C-NMR (101 MHz, chloroform-d, *δ*, ppm): 170.10, 158.43, 158.12, 157.87, 146.84, 140.01, 137.84, 136.49, 135.22, 134.18, 130.50, 130.25 (d, *J*=10.8 Hz), 129.65, 127.94 (d, *J*=11.5 Hz), 126.98, 117.33, 114.07, 113.76, 113.40, 55.23 (d, *J*=2.8 Hz), 50.71, 35.07, 34.02, 31.42, 29.49. ESI-MS (*m/z*): calcd. for $C_{48}H_{49}NO_2$: 671.38; Found 671.40 [M]$^+$.

All the complexes were prepared in a similar method. Taking **Co6** for instance, to a stirred solution of the **L6** (0.4 mmol) at room temperature, an ethanol solution containing 0.5 equiv. of $Co(OAc)_2{\cdot}4H_2O$ (0.2 mmol, 0.055 g) reaction mixture

https://doi.org/10.1007/s10118-022-2758-5

was refluxed for 24 h and cooled down to room temperature. The resultant precipitate was filtered, subsequently washed with hexane, and dried in vacuo at 40 °C overnight finally affording brown powder.

Co1. Yield 64.3%. FTIR (KBr, cm^{-1}): 2952, 2832, 1616(ν(C=N)), 1507, 1455, 1438, 1359, 1300, 1246, 1173, 1105, 1032, 868, 830, 768,734, 669, 576. Anal. Calcd. for $C_{104}H_{112}CoN_2O_{10}$: C, 77.64 H, 7.02 N,1.74. Found: C, 77.18 H, 7.17 N, 1.65. ESI-MS (*m/z*): required 1608.98; Found 1608.9035 $[M]^+$.

Co2. Yield 68.4%. FTIR (KBr, cm^{-1}): 2956, 2866, 1891, 1619(ν(C=N), 1503, 1434, 1356, 1225, 1153, 1118, 1095, 1012, 974, 830, 796, 723, 565. Anal. Calcd. for $C_{96}H_{88}CoF_8N_2O_2$: C, 76.23 H, 5.86 N, 1.85. Found: C, 76.14 H, 5.7 N, 1.74. ESI-MS (*m/z*): required 1512.69; Found 1512.0365 $[M]^+$.

Co3. Yield 65.2%. FTIR (KBr, cm^{-1}): 2953, 2926, 2860, 1618(ν(C=N)), 1506, 1436, 1245, 1196, 1169, 1121, 1021, 984, 870, 806, 726, 665, 569. Anal. Calcd. for $C_{104}H_{112}CoN_2O_2$: C, 84.35 H, 7.62 N, 1.89. Found: C, 84.07 H, 7.43 N, 1.78. ESI-MS (*m/z*): required 1480.99; Found 1480.3930 $[M]^+$.

Co4. Yield 60.1%. FTIR (KBr, cm^{-1}): 2956, 2867, 1621(ν(C=N)), 1587, 1506, 1436, 1351, 1252, 1165, 1111, 1021, 874, 813, 767, 720, 662, 569. Anal. Calcd. for $C_{110}H_{124}CoN_2O_2$: C, 84.41 H, 7.99 N, 1.79. Found: C, 84.08 H, 7.47 N, 1.75. ESI-MS (*m/z*): required 1565.15; Found 1565.0721 $[M]^+$.

Co5. Yield 67.6%. FTIR (KBr, cm^{-1}): 2953, 2863, 1618(ν(C=N)), 1570, 1502, 1450, 1313, 1248, 1193, 1165, 1131, 1049, 867, 840, 813, 760, 720, 672, 569. Anal. Calcd. for $C_{104}H_{112}CoN_2O_5$: C, 81.70 H, 7.38 N, 1.83. Found: C, 81.16 H, 7.22 N, 1.73. ESI-MS (*m/z*): required 1528.98; Found 1528.7744 $[M]^+$.

Co6. Yield 63.9%. FTIR (KBr, cm^{-1}): 2953, 2826, 1618(ν(C=N)), 1574, 1489, 1457, 1313, 1252, 1193, 1169, 1135, 1049, 1031, 840, 760, 699, 596. Anal. Calcd. for $C_{96}H_{96}CoN_2O_4$: C,82.32 H, 6.91 N, 2.00. Found: C, 82.11 H, 6.35 N, 1.95. ESI-MS (*m/z*): required 1400.77; Found 1400.6528 $[M]^+$.

Polymerization of Butadiene

A typical procedure for the polymerization is as follows: a toluene (10 mL) solution of 1,3-butadiene (1 g, 0.0185 mol) was added to a moisture free ampule bottle preloaded with complex **Co6** (2.5 mg, 0.0018 mmol), then EASC (0.54 mmol) was injected to initiate the polymerization at 50 °C. After 24 h, methanol was added to the system to quench the polymerization. The mixture was poured into a large quantity of methanol containing 2,6-di-*tert*-butyl-4-methylphenol (1.0 wt%) as a stabilizer. Filtered and dried under vacuum at 40 °C, polybutadiene was resulted at a con-stant weight (0.92 g, 92%). We chose EASC($Al_2Et_3Cl_3$) as the co-catalyst and **Co6** as the main catalyst to optimize the polymerization conditions.

RESULTS AND DISCUSSION

Synthesis and Characterization of the Cobalt Complexes Co1–Co6

The salicylaldimine ligands **L1**–**L6** bearing bulky substituted benzhydryl groups were prepared in high yields by condensation reaction between 3,5-di(*tert*-butyl)salicylaldehyde and 1.0 equiv. of aniline derivatives. Subsequent coordination with $Co(OAc)_2{\cdot}4H_2O$ in refluxing ethanol afforded the targeted complexes **Co1**–**Co6** (Scheme 1). All the ligands were well identified by ^{1}H-NMR, ^{13}C-NMR, FTIR analysis, and the cobalt complexes were characterized by FTIR and elemental analysis. In order to establish the coordination environment around the metal center, single crystal of complex **Co6** was successfully isolated (Fig. 1), and its selective bond distances and angles and crystallographic details are shown in Table S1 and S2 (in the electronic supplementary information, ESI). Moreover, to confirm the steric bulky nature at the metal center in **Co6** and highlight its differences after incorporating benzhydryl moieties, comparisons with its structurally similar analogues bearing different 2,6-disubstituted anilinyl groups, *i.e.*, 2,6-^{i}Pr$_2$ for complex *N*-(2,6-diisopropylanilinyl)salicylaldiminate cobalt (**Co$_{iPr}$**) and 2,6-H_2 for complex *N*-(4-methoxylanilinyl)salicylaldiminate cobalt (**Co$_H$**), were also implemented.[54,55]

Single crystal of complex **Co6** was isolated by layering Et_2O onto its saturated dichloromethane solution. As the structure shown in Fig. 1, the cobalt center is coordinated by two bidentate salicylaldiminate ligands, and its coordination geo-

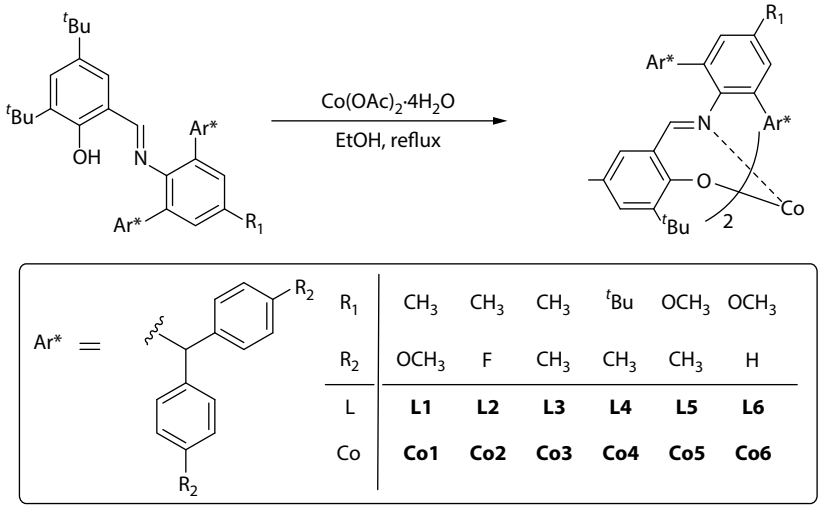

R_1	CH_3	CH_3	CH_3	^{t}Bu	OCH_3	OCH_3
R_2	OCH_3	F	CH_3	CH_3	CH_3	H
L	**L1**	**L2**	**L3**	**L4**	**L5**	**L6**
Co	**Co1**	**Co2**	**Co3**	**Co4**	**Co5**	**Co6**

Scheme 1 Synthesis procedure for cobalt complexes **Co1**–**Co6**.

https://doi.org/10.1007/s10118-022-2758-5

metry can be best described as *pseudo*-tetrahedral. The Co—O and Co—N bond distances are 1.9178(14) Å and 2.0030(16) Å, respectively, which are obviously longer than other reported bis(salicylaldiminate) Co(II) complexes that generally revealed Co—O bond distances of 1.87–1.91 Å and Co—N of 1.96–2.03 Å (Table 1). Such a structural difference was probably due to the presence of steric bulky benzhydryl groups on the ligand, which repelled each other to avoid steric overlapping.[56–61] Probably because of the same reason, the cobalt atom deviated from the salicylaldimine plane constructed by (O2, C40, C35, C34, N1) by a value of 0.590 Å, which was much greater than those in other reported bis(salicylaldiminate) Co(II) complexes, in which the cobalt atom was generally located on such a plane.[56–61]

Besides the above structure differences, the steric bulky nature around the metal center in **Co6** can be also reflected from its space-filling model. Fig. 2 demonstrates its space-filling difference with complexes $\mathbf{Co_{iPr}}$ and $\mathbf{Co_H}$,[54,55] from which it can be clearly observed that the cobalt atom in **Co6** is buried tightly in its surrounded ligand skeletons, leaving only one "cavity" for further reactions; whereas for $\mathbf{Co_{iPr}}$ and $\mathbf{Co_H}$, the metal centers are more exposed, giving them more reaction possibilities with outer-accessed substrates. The same conclusion can be also drawn from an alternative parameter of the buried volume (V_{bur}),[62–64] which has been extensively used to evaluate the steric environments around the metal center.[65–67] As shown in Fig. 3, the V_{bur} value of cobalt atom in **Co6** (44.7%) is significantly higher than those in $\mathbf{Co_{iPr}}$ (40.6%) and $\mathbf{Co_H}$ (38.6%), indicative of the more bulky nature for the cobalt atom in **Co6**. Because of this unprecedent bulky characteristic, the formed active species in **Co6** can be well protected from impurities from the polymerization medium, and therefore brings a much higher Catalytic efficiency (*vide infra*).

1,3-Butadiene Polymerization Performances

Cobalt complexes have been extensively evaluated as high *cis*-

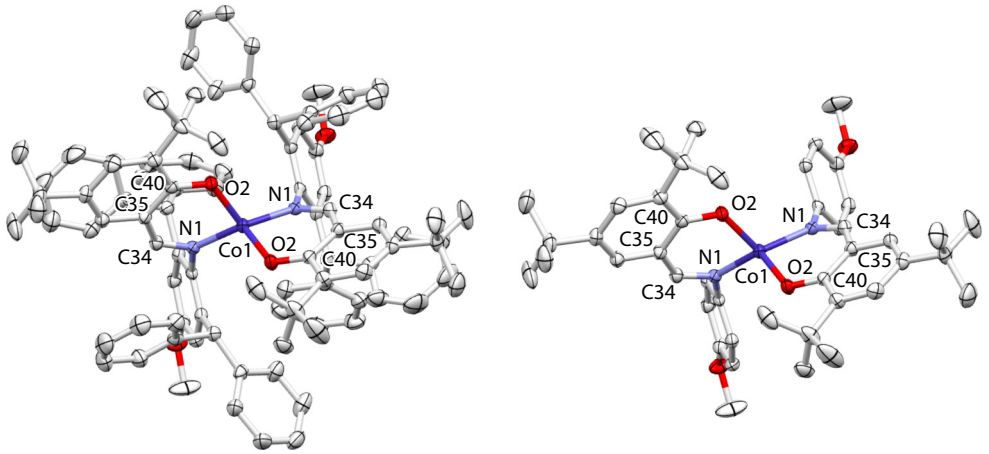

Fig. 1 Single-crystal structure of complex **Co6** with with 50% probability thermal ellipsoids (in the right figure, benzhydryl moieties were omitted for clarity).

Table 1 Bond distance differences between **Co6** and other reported bis(salicylaldiminate) Co(II) complexes.

Complex	Co—O (Å)	Co—N (Å)	Complex	Co—O (Å)	Co—N (Å)
Co6	1.9178(14)	2.0030(16)	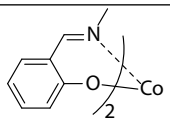	1.859(5)	1.983(6) [57]
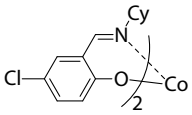	1.892	1.988 [56]	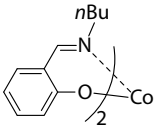	1.898(2) 1.902(2)	1.967(3) 1.975(3) [59]
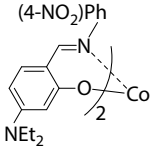	1.909	1.997(2) [61]	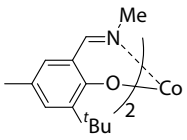	1.879 1.872	2.034 2.002 [58]
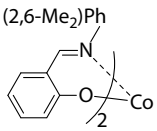	1.895	1.968 [60]	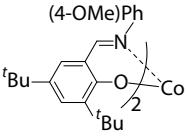	1.890(3) 1.892(3)	1.979(4) 1.988(4) [54]

https://doi.org/10.1007/s10118-022-2758-5

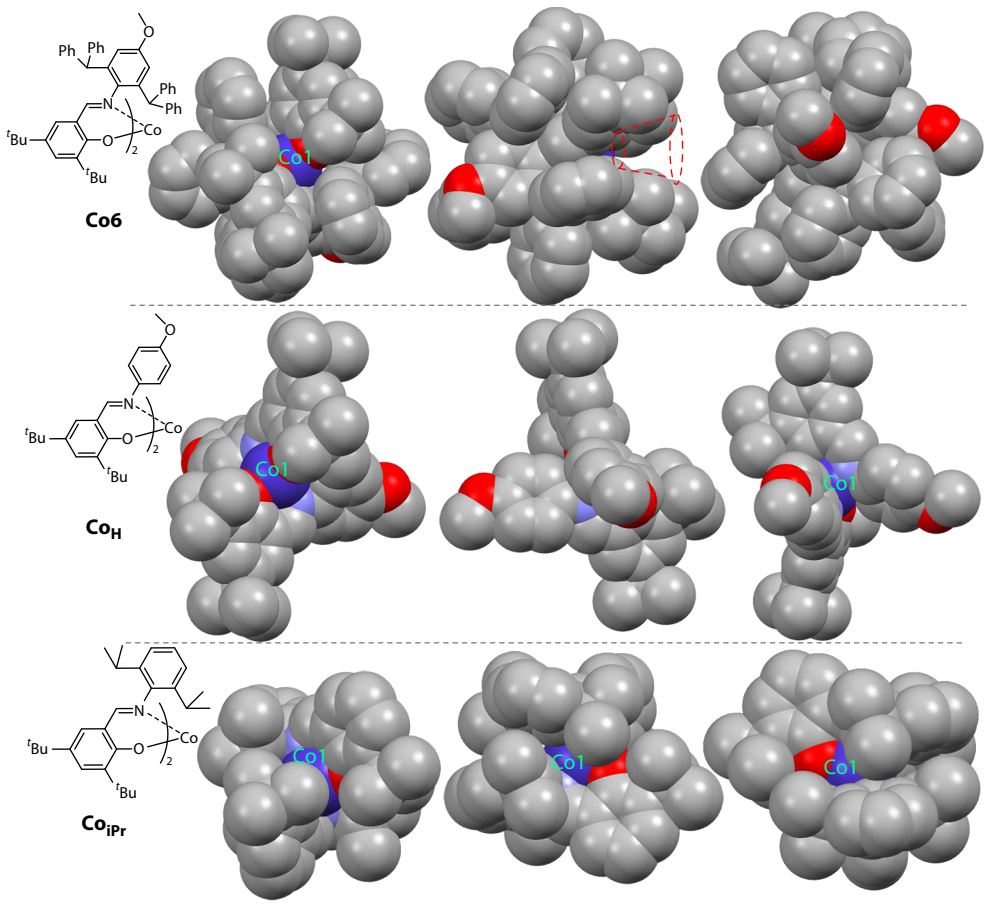

Fig. 2 Front, side and back views (from left to right) of the spacefilling model of complex **Co6** (top), $\mathbf{Co_H}$ (middle),[54] $\mathbf{Co_{iPr}}$ (bottom).[55]

1,4-selective catalysts for 1,3-butadiene polymerization. Nevertheless, for most of these studies, comparatively higher precatalyst loading is generally required if good polymer yields are desired (*vide supra*). Considering the unique bulky nature around the cobalt atoms for the present complexes, when low catalyst loading was applied for the polymerization, the active species can be well protected from possible impurities in the reaction medium, and therefore is anticipated to work well in such a condition. Based on these considerations, complex **Co6** was selected as a representative precatalyst for subsequent 1,3-butadiene polymerization at low catalyst concentrations. In order to explore the limiting value of the catalytic efficiency, low catalytic loading with a ratio of [BD]/**Co6** in the range of 5×10^4–2×10^5 was mainly investigated. It is of note that, when extremely low precatalyst concentration was applied, increased aluminum alkyl compounds are generally required to scavenge impurities, therefore, relative higher cocatalyst ratios of [EASC]/**Co6** are applied in the present studies. As the results shown in Table 2, initial evaluation of 1,3-butadiene polymerization at a ratio of [BD]/**Co6**=5×10^4 give satisfying results. In the presence of 100 equiv. of EASC, the polymer yield could reach as high as 77%, and this value can be further improved to 92% when 300 equiv. of EASC was applied. Continuous decreasing the precatalyst concentration to [BD]/**Co6**=8×10^4 led to a slightly decreased yield of 71%, and again, such a yield can be improved to 81% when further increasing the EASC equivalents to 500. These results clearly indicated the high catalytic efficiencies of the formed active species, that were guaranteed by the bulky nature of the salicylaldimine ligands. Moreover, it was also found that, complex **Co6** could successfully maintain to be active at ratios of [BD]/**Co6**=1×10^5 and 2×10^5, which, to the best of our knowledge, were the lowest catalyst concentrations that have been reported, although much lower polymer yields were revealed.

For a typical coordination polymerization, the molecular weights of the resultant polymers are generally reversely related to the concentrations of precatalyst, *i.e.*, a lower concentration of precatalyst usually generates comparatively higher molecular weights. Nevertheless, for **Co6** mediated systems, although their catalyst concentrations were much lower, the resultant molecular weights of polybutadienes were very similar to other Co(II) mediated diene polymerizations in which a range of molecular weights M_n=10.0×10^4–30.0×10^4 were obtained at high precatalyst concentrations. Such unusual results were probably caused by the chain transfer reactions to aluminum compounds. Due to the presence of excessive amounts of cocatalyst EASC in **Co6** mediated polymerizations, chain transfer to EASC was greatly facilitated and therefore played a larger role in reducing the molecular weights of

https://doi.org/10.1007/s10118-022-2758-5

polybutadienes, which eventually gave rise to comparable molecular weights. Similar chain transfer reactions to alkyl aluminum chloride compounds was reported in many other Co(II) promoted diene polymerizations.[68] Inspired by the above high catalytic efficiencies of **Co6** at low catalyst concentrations, other cobalt complexes **Co1**–**Co5** were also evaluated at similar conditions to establish the structure-reactivity relationship. As the results shown in Table 3, all the other five complexes reveal comparable high activities to **Co6** at a ratio of [BD]/[Co]=5×10^4, indicating the universal high catalytic efficiency caused by positive shielding effect of benzhydryl groups. Moreover, varying the substituents on benzhydryl moieties seemed to bring little influence on the catalytic activities, and all the polymer yields were around 90%. These results can be explained from the similarity of the buried volume (V_{bur}), as revealed the topographical steric maps of the structures of **Co1**–**Co6** that were optimized by DFT calculations (Fig. 4). Due to the remote distances of R_1 and R_2, varying these substituents brought subtle influence on the coordination/insertion environment around the active species,

Table 2 1,3-Butadiene polymerization under different conditions using **Co6**. [a]

Run	BD/**Co6**	EASC/Co	Yield (wt%)	M_n (×10^4) [b]	M_w/M_n	Microstructure [c] (%)		
						Cis-1,4	*Trans*-1,4	1,2
1	50000	100	77	11.1	1.7	87.2	11.0	1.8
2	50000	300	92	8.2	2.5	84.5	13.5	2.0
3	80000	300	71	11.8	2.0	88.4	9.6	2.0
4	80000	500	81	18.8	2.9	85.3	11.6	3.1
5	100000	300	39	20.1	2.4	84.7	12.6	2.7
6	100000	500	70	29.1	2.2	84.3	11.6	4.1
7	200000	300	29	20.1	5.6	81.6	15.8	2.6
8	200000	500	48	14.9	7.5	86.2	11.6	2.2

[a] Polymerization conditions: in toluene for 24 h at 50 °C, [Bd]=1.85 mol/L, EASC: ethylaluminum sesquichloride; [b] Determined by GPC eluted with THF (polystyrenes as standards); [c] Determined by FTIR.

Table 3 1,3-Butadiene polymerization of complexes **Co1**–**Co6**. [a]

Run	Cat.	EASC/Co	Yield (wt%)	M_n (×10^4) [b]	M_w/M_n	Microstructure [c] (%)		
						Cis-1,4	*Trans*-1,4	1,2
1	**Co1**	300	92	13.1	2.4	93.8	3.9	2.3
2	**Co2**	300	90	6.6	2.4	92.7	5.6	1.7
3	**Co3**	300	91	13.1	2.7	93.9	4.3	1.8
4	**Co4**	300	89	16.7	2.4	92.5	5.9	1.6
5	**Co5**	300	93	8.8	2.9	88.7	9.0	2.3
6	**Co6**	300	92	8.2	2.5	84.5	13.5	2.0

[a] Polymerization conditions: in toluene for 24 h at 50 °C, [Bd] = 1.85 mol/L, [BD]/[Co] = 50000; [b] Determined by GPC eluted with THF (polystyrenes as standards); [c] Determined by IR.

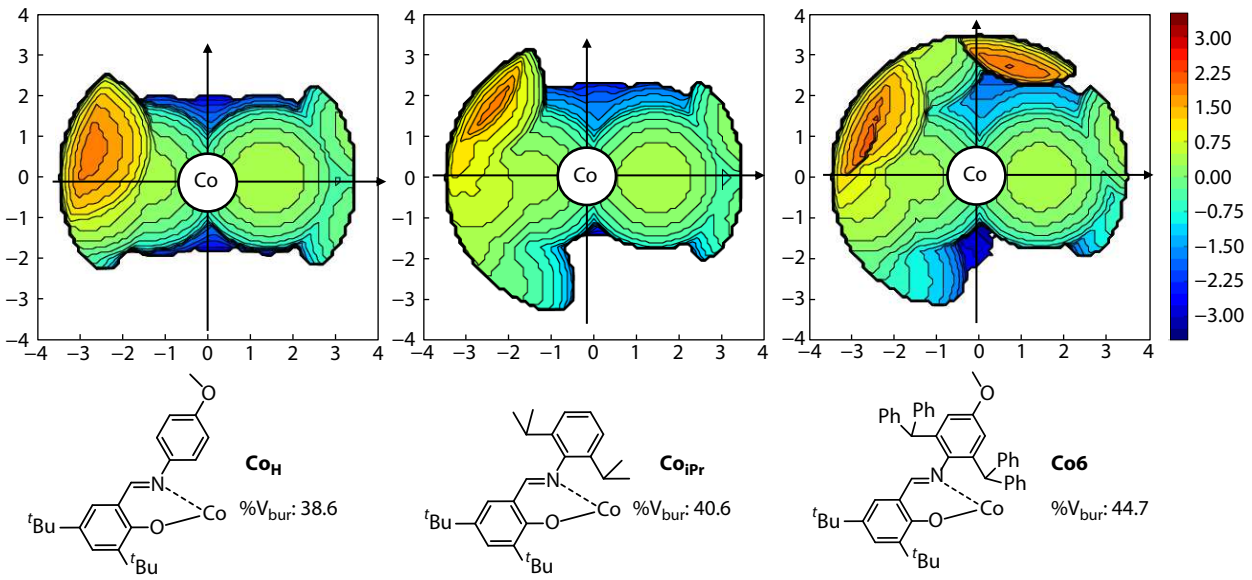

Fig. 3 Topographical steric maps and percent of buried volume (V_{bur}) for complexes **Co$_H$** (left),[54] **Co$_{iPr}$** (middle)[55] and **Co6** (right) (only one salicylaldimine ligand was taken into account to be consistent with the hypothesized active species that contains only one ligand[43]).

https://doi.org/10.1007/s10118-022-2758-5

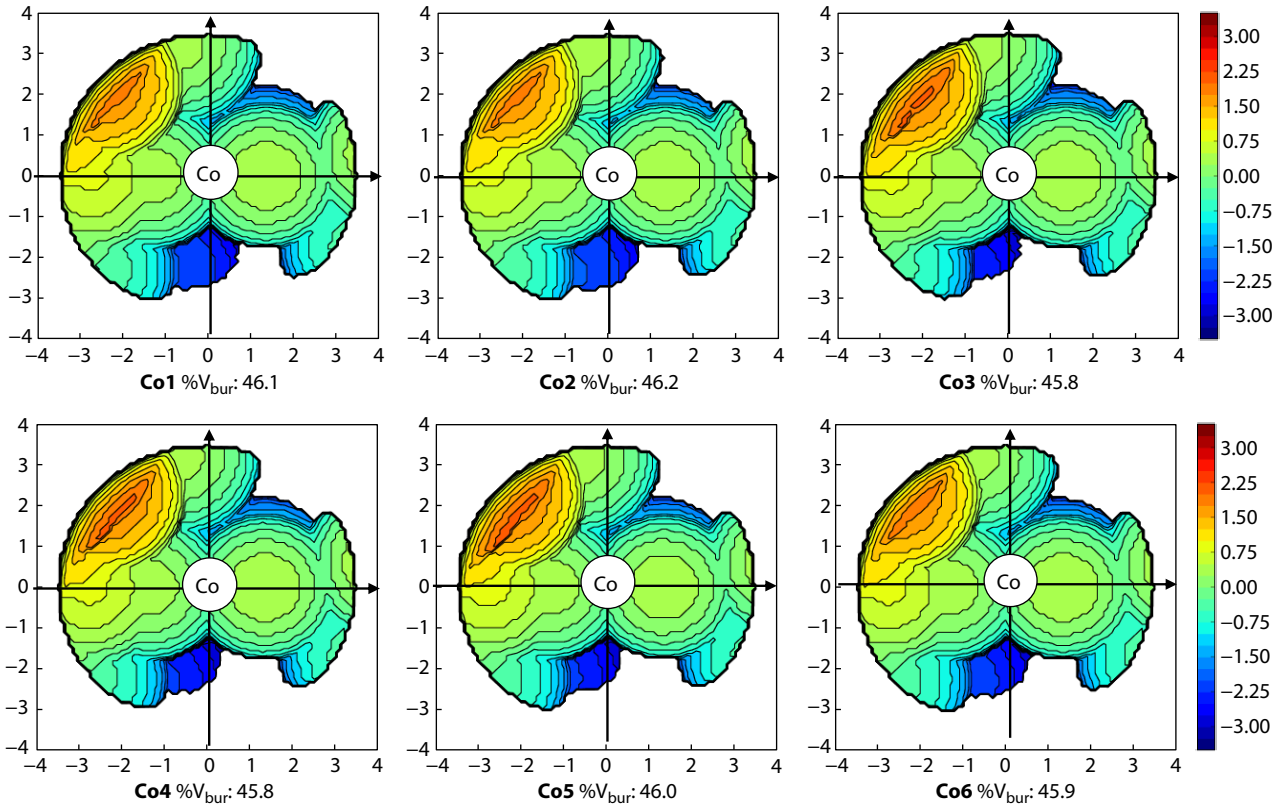

Fig. 4 Topographical steric maps and percent of buried volume (V_{bur}) for the structures of **Co1**–**Co6** that were optimized by DFT calculations (only one salicylaldimine ligand was taken into.

and therefore, very similar catalytic activities were given eventually. Nevertheless, ligand structures imposed significant influence on the molecular weights of the resultant polybutadienes. These results might be relevant to both steric and electronic effects. As indicated above, due to the presence of excessive amount of EASC, chain transfer to aluminum played a pivotal role in governing the molecular weights, therefore, any factors that were beneficial to chain transfer reactions would result in smaller molecular weights. Generally, chain transfer to aluminum occurs through a bimetallic Co-Al intermediate and decreasing the steric bulkiness and enhancing the electropositivity at the metal center suppresses favors greatly the formation of such bimetallic intermediate. Based on this consideration, *tert*-butyl groups on the outer space of complex **Co4** would retard the accessing of EASC to the cobalt center to generate bimetallic intermediate, and eventually resulted in much higher molecular weight (16.7×10^4); for complex **Co2** bearing strong electro-withdrawing fluoro-group on the *N*-phenyl moiety, a more positive charge on the cobalt center would be revealed, that was in favor of the formation of bimetallic intermediate, and eventually, resulted in the smallest molecular weight (6.6×10^4). After combining the steric and electronic reasons, a general trend of **Co4** > **Co1**~**Co3** > **Co5**~**Co6** > **Co2** was demonstrated in our studies. Regarding the microstructure of the afforded polybutadienes, **Co1**, **Co2**, **Co3** and **Co4** gave much similar *cis*-1,4-contents that were in the range of 92.9%–93.9%, however, **Co5** and **Co6** demonstrated much lower *cis*-1,4-selectivities. Currently, specific reasons for these results were still unclear yet, but might be relative to the strong electron-donating ability of MeO— groups, that is unfavorable for the 1,3-butadiene monomer to coordinate the metal center in a *cis*-η^4 fashion.

Increasing the axial bulkiness of late-transition metal complexes could enhance their thermostabilities during olefin polymerizations.[23,69–73] For the present cobalt complexes **Co1**–**Co6**, significantly increased bulkiness is also provided by the benzhydryl moieties, therefore, their catalytic thermostabilities for 1,3-butadiene polymerization were also evaluated. Initial studies revealed that conducting the polymerization at extreme low precatalyst concentrations ([Bd]/[Co]= 5×10^4) gave much poor catalytic activities at high temperature of 120 °C, therefore, during the subsequent thermostability studies, all the polymerizations were implemented at a decreased ratio of [BD]/[Co] = 1×10^4, and for such a ratio, the cocatalyst loading could be lowered to a common value of 10. As the results summarized in Table 4 and Fig. 5, the six cobalt complexes **Co1**–**Co6** demonstrated very high catalytic efficiencies at relative lower temperatures of 30 and 50 °C, giving very high polymer yields. Increasing the polymerization temperature to 80 °C brought little influence on the catalytic activities, and all the polymer yields were higher than 80%, indicative of the high thermostabilities of the corresponding cobalt active species that were enhanced by the bulky benzhydryl moieties. Moreover, it was also satisfying to find that all the six complexes could successfully survive at a temperature as high as 120 °C, which confirmed again the

Table 4 1,3-Butadiene polymerization by **Co1**–**Co6** at different temperatures.[a]

Run	Cat.	T (°C)	Yield (wt%)	M_n ($\times10^4$) [b]	M_w/M_n	Microstructure [c] (%)		
						Cis-1,4	*Trans*-1,4	1,2
1	**Co1**	30	88	29.5	2.1	95.6	3.1	1.3
2		50	93	16.4	3.0	91.7	5.8	2.3
3		80	88	8.1	3.9	83.5	12.0	4.5
4		120	62	9.9	3.3	79.7	15.2	5.1
5	**Co2**	30	81	27.3	2.1	95.4	3.2	1.4
6		50	87	13.5	3.1	92.2	5.7	2.1
7		80	90	9.3	3.9	84.0	12.3	3.7
8		120	70	9.2	3.8	80.1	16.0	3.9
9	**Co3**	30	82	27.3	2.0	95.2	3.3	1.5
10		50	90	16.2	3.1	91.3	6.7	2.0
11		80	86	8.2	3.8	82.7	13.1	4.2
12		120	78	10.6	3.1	83.6	12.8	3.6
13	**Co4**	30	74	28.3	2.0	95.0	3.8	1.2
14		50	94	13.4	3.1	92.0	5.8	2.2
15		80	89	8..8	4.0	81.4	15.0	3.6
16		120	77	7.1	3.8	82.7	13.0	4.3
17	**Co5**	30	82	30.0	2.0	96.4	2.3	1.3
18		50	97	8.1	4.1	91.0	5.9	3.1
19		80	87	7.2	4.5	84.5	10.5	5.0
20		120	74	8.0	3.3	82.7	12.3	5.0
21	**Co6**	30	93	35.0	2.3	95.8	3.0	1.2
22		50	100	19.2	2.4	89.7	8.4	1.9
23		80	83	8.8	4.0	83.2	13.9	2.9
24		120	86	7.0	3.8	78.1	17.8	4.1

[a] Polymerization conditions: in toluene for 3 h, [Bd]/[Co]=1×10^4, [Al]/[Co]=10, [Bd] = 1.85 mol/L; [b] Determined by GPC eluted with THF (polystyrenes as standards); [c] Determined by FTIR.

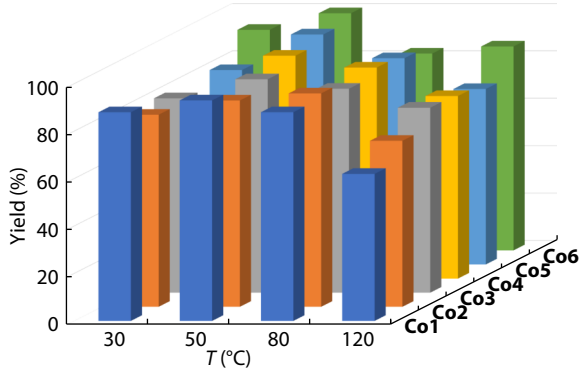

Fig. 5 Polymer yields of different cobalt complexes **Co1**–**Co6** at 30 °C, 50 °C, 80 °C and 120 °C.

thermal robustness of the active species. Increasing the polymerization temperature imposed significant influence on the molecular weight as well as the microstructures of the resultant polybutadiene products. Generally, elevating temperature would facilitate the chain transfer reactions, that gave rise to gradually decreased molecular weights; and at higher temperature, the growing polybutadienyl propagating active species would shift from an *anti*-η^3 to a *syn*-η^3, and eventually more *trans*-1,4- content would be generated from the latter configuration.

CONCLUSIONS

A family of bis(salicylaldiminate) Co(II) complexes are synthesized and their catalytic performances towards butadiene polymerization is reported herein. Due to the highly bulky nature of the ligands that are caused by the steric congested benzhydryl moieties, the cobalt metal centers can be well protected from any possible impurities, and therefore, the complexes reveal ultra-high catalytic efficiencies even at extreme low catalyst concentrations. At a ratio of [BD]/[Co] = 5×10^4, all the complexes could well catalyze 1,3-butadiene polymerizations, giving polymer yields higher than 90%. Ligand structures brought little influence on the catalytic activities but influenced significantly the molecular weights of the resultant polybutadienes, giving an order of **Co4** > **Co1**~**Co3** > **Co5**~**Co6** > **Co2**, that is relevant to chain transfer efficiencies. In addition, such a highly bulky nature also brings in significantly enhanced thermostabilities of the active species, that give quite high polymer yields at temperatures up to 120 °C, implying the positive influence of congested benzhydryl moiety in achieving thermo robust catalysts. Nevertheless, increasing the polymerization temperature resulted in gradually decreased molecular weights and *cis*-1,4- contents due to the facilitated chain transfer and *anti-syn* isomerization of the active species.

ASSOCIATED CONTENT

Crystallographic data for **Co6**

CCDC 2132656 contains the supplementary crystallographic data for this work. These data can be obtained free of charge *via* www.ccdc.cam.ac.uk/data_request/cif, or by emailing data_request@ccdc.cam.ac.uk, or by contacting The Cambridge Crystallographic Data Centre, 12 Union Road, Cambridge CB2 1EZ, UK; fax: +44 1223 336033

https://doi.org/10.1007/s10118-022-2758-5

NOTES

The authors declare no competing financial interest.

Electronic Supplementary Information

Electronic supplementary information (ESI) is available free of charge in the online version of this article at http://doi.org/10.1007/s10118-022-2758-5.

ACKNOWLEDGMENTS

This work was financially supported by the National Natural Science Foundation of China (Nos. U1862206 and 21801236).

REFERENCES

1 Guan, Z.; Popeney, C. Recent progress in late transition metal α-diimine catalysts for olefin polymerization. *Top. Organomet. Chem.* **2009**, *26*, 179–220.
2 Chen, C. Designing catalysts for olefin polymerization and copolymerization: beyond electronic and steric tuning. *Nat. Rev. Chem.* **2018**, *2*, 6–14.
3 Liang, T.; Goudari, S. B.; Chen, C. A simple and versatile nickel platform for the generation of branched high molecular weight polyolefins. *Nat. Commun.* **2020**, *11*, 372.
4 Chen, M.; Chen, C. Direct and tandem routes for the copolymerization of ethylene with polar functionalized internal olefins. *Angew. Chem. Int. Ed.* **2020**, *59*, 1206–1210.
5 Dai, S.; Chen, C. Direct synthesis of functionalized high-molecular-weight polyethylene by copolymerization of ethylene with polar monomers. *Angew. Chem. Int. Ed.* **2016**, *55*, 13281–13285.
6 Jian, Z.; Falivene, L.; Boffa, G.; Sánchez, S. O.; Caporaso, L.; Grassi, A.; Mecking, S. Direct synthesis of telechelic polyethylene by selective insertion polymerization. *Angew. Chem. Int. Ed.* **2016**, *55*, 14378–14383.
7 Hu, X.; Kang, X.; Zhang, Y.; Jian, Z. Facile access to polar-functionalized ultrahigh molecular weight polyethylene at ambient conditions. *CCS Chem.* **2021**, *3*, 2598–1612.
8 Wang, C.; Zhang, Y.; Mu, H.; Jian, Z. Systematic studies on dibenzhydryl and pentiptycenyl substituted pyridine-imine nickel(II) mediated ethylene polymerization. *Dalton Trans.* **2020**, *49*, 4824–4833.
9 Suo, H.; Solan, G. A.; Ma, Y.; Sun, W. H. Developments in compartmentalized bimetallic transition metal ethylene polymerization catalysts. *Coord. Chem. Rev.* **2018**, *372*, 101–116.
10 Wang, Z.; Solan, G. A.; Zhang, W.; Sun, W. H. Carbocyclic-fused *N*,*N*,*N*-pincer ligands as ring-strain adjustable supports for iron and cobalt catalysts in ethylene oligo-/polymerization. *Coord. Chem. Rev.* **2018**, *363*, 92–108.
11 Ma, J.; Feng, C.; Wang, S.; Zhao, K. Q.; Sun, W. H.; Redshaw, C.; Solan, G. A. Bi- and tri-dentate imino-based iron and cobalt pre-catalysts for ethylene oligo-/polymerization. *Inorg. Chem. Front.* **2014**, *1*, 14–34.
12 Cheng, H.; Wang, H.; Li, Y.; Hu, Y.; Zhang, X.; Cai, Z. Structurally simple dinuclear nickel catalyzed olefin copolymerization with polar monomers. *J. Catal.* **2018**, *368*, 291–297.
13 Li, Y.; Cheng, H.; Xiao, R.; Cai, Z. Rational design of nickel catalysts containing *N*-acylated imidazolin-2-imine ligand for ethylene copolymerization with polar monomer. *J. Catal.* **2020**, *383*, 117–123.
14 Fu, X.; Zhang, L.; Tanaka, R.; Shiono, T.; Cai, Z. Highly robust nickel catalysts containing anilinonaphthoquinone ligand for copolymerization of ethylene and polar monomers. *Macromolecules* **2017**, *50*, 9216–9221.
15 Li, M.; Shu, X.; Cai, Z.; Eisen, M. S. Synthesis, structures, and norbornene polymerization behavior of neutral nickel(II) and palladium(II) complexes bearing aryloxide imidazolidin-2-imine ligands. *Organometallics* **2018**, *37*, 1172–1180.
16 Zhong, L.; Zheng, H.; Du, C.; Du, W.; Liao, G.; Cheung, C. S.; Gao, H. Thermally robust α-diimine nickel and palladium catalysts with constrained space for ethylene (co)polymerizations. *J. Catal.* **2020**, *384*, 208–217.
17 Zhong, S.; Tan, Y.; Zhong, L.; Gao, J.; Liao, H.; Jiang, L.; Gao, H.; Wu, Q. Precision synthesis of ethylene and polar monomer copolymers by palladium-catalyzed living coordination copolymerization. *Macromolecules* **2017**, *50*, 5661–5669.
18 Guo, L.; Gao, H.; Guan, Q.; Hu, H.; Deng, J.; Liu, J.; Liu, F.; Wu, Q. Substituent effects of the backbone in α-diimine palladium catalysts on homo- and copolymerization of ethylene with methyl acrylate. *Organometallics* **2012**, *31*, 6054–6062.
19 Ying, W.; Pan, W.; Gan, Q.; Jia, X.; Grassi, A.; Gong, D. Preparation and property investigation of chain end functionalized *cis*-1,4 polybutadienes *via* de-polymerization and cross metathesis of *cis*-1,4 polybutadienes. *Poly. Chem.* **2019**, *10*, 3525–3534.
20 Liang, S.; Zhang, H.; Cong, R.; Liu, H.; Wang, F.; Hu, Y.; Zhang, X. In-chain functionalized syndiotactic 1,2-polybutadiene by a Ziegler-Natta iron(III) catalytic system. *RSC Adv.* **2019**, *9*, 33465–33471.
21 Li, G.; Xu, G.; Ge, Y.; Dai, S. Synthesis of fluorinated polyethylene of different topologies *via* insertion polymerization with semifluorinated acrylates. *Poly. Chem.* **2020**, *11*, 6335–6342.
22 Dai, S.; Li, G.; Lu, W.; Liao, Y.; Fan, W. Suppression of chain transfer *via* a restricted rotation effect of dibenzosuberyl substituents in polymerization catalysis. *Polym. Chem.* **2021**, *12*, 3240–3249.
23 Lu, Z.; Chang, G.; Wang, H.; Jing, K.; Dai, S. A dual steric enhancement strategy in α-diimine nickel and palladium catalysts for ethylene polymerization and copolymerization. *Organometallics* **2022**, *41*, 124–132.
24 Na, Y.; Dai, S.; Chen, C. Direct synthesis of polar-functionalized linear low-density polyethylene (LLDPE) and low-density polyethylene (LDPE). *Macromolecules* **2018**, *51*, 4040–4048.
25 Lian, K.; Zhu, Y.; Li, W.; Dai, S.; Chen, C. Direct synthesis of thermoplastic polyolefin elastomers from nickel-catalyzed ethylene polymerization. *Macromolecules* **2017**, *50*, 6074–6080.
26 Ricci, G.; Pampaloni, G.; Sommazzi, A.; Masi, F. Dienes polymerization: where we are and what lies ahead. *Macromolecules* **2021**, *54*, 5879–5941.
27 Ricci, G.; Sommazzi, A.; Masi, F.; Ricci, M.; Boglia, A.; Leone, G. Well-defined transition metal complexes with phosphorus and nitrogen ligands for 1,3-dienes polymerization. *Coord. Chem. Rev.* **2010**, *254*, 661–676.
28 Gong, D.; Wang, B.; Bai, C.; Bi, J.; Wang, F.; Dong, W.; Zhang, X.; Jiang, L. Metal dependent control of *cis*-/*trans*-1,4 regioselectivity in 1,3-butadiene polymerization catalyzed by transition metal complexes supported by 2,6-bis[1-(iminophenyl)ethyl]pyridine. *Polymer* **2009**, *50*, 6259–6264.
29 Pan, W.; Chen, H.; Mu, J.; Li, W.; Jiang, F.; Weng, G.; Hu, Y.; Gong, D.; Zhang, X. Synthesis of high crystalline syndiotactic 1,2-polybutadienes and study on their reinforcing effect on *cis*-1,4 polybutadiene. *Polymer* **2017**, *111*, 20–26.
30 Gong, D.; Dong, W.; Hu, Y.; Bi, J.; Zhang, X.; Jiang, L. Syndiotactically enriched 1,2-selective polymerization of 1,3-butadiene initiated by iron catalysts based on a new class of donors. *Polymer* **2009**, *50*, 5980–5986.
31 Liu, H.; Jia, X.; Wang, F.; Dai, Q.; Wang, B.; Bi, J.; Zhang, C.; Zhao, L.; Bai, C.; Hu, Y.; Zhang, X. Synthesis of bis(*N*-arylcarboximidoylchloride)pyridine cobalt(II) complexes and

their catalytic behavior for 1,3-butadiene polymerization. *Dalton Trans.* **2013**, *42*, 13723–13732.
32 Liu, H.; Yang, S. Z.; Wang, F.; Bai, C. X.; Hu, Y. M.; Zhang, X. Q. Polymerization of 1,3-butadiene catalyzed by cobalt(II) and nickel(II) complexes bearing pyridine-2-imidate ligands. *Chinese J. Polym. Sci.* **2016**, *34*, 1060–1069.
33 Fang, L.; Zhao, W. P.; Han, C.; Zhan, C. Y.; Liu, H.; Hu, Y. M.; Zhang, X. Q. 1,3-Butadiene polymerizations catalyzed by cobalt and iron dichloride complexes bearing pyrazolylimine ligands. *Chinese J. Polym. Sci.* **2019**, *37*, 462–470.
34 Nath, D. C. D.; Shiono, T.; Ikeda, T. Additive effect of triphenylphosphine on the living polymerization of 1,3-butadiene with a cobalt dichloride-methylaluminoxane catalytic system. *Macromol. Chem. Phys.* **2003**, *204*, 2017–2022.
35 Nath, D. C. D.; Shiono, T.; Ikeda, T. Copolymerization of 1,3-butadiene and isoprene with cobalt dichloride/methylaluminoxane in the presence of triphenylphosphine. *J. Polym. Sci., Part A: Polym. Chem.* **2002**, *40*, 3086–3092.
36 Deb Nath, D. C.; Shiono, T.; Ikeda, T. Polymerization of 1,3-butadiene by cobalt dichloride activated with various methylaluminoxanes. *Appl. Catal. A-Gen.* **2003**, *238*, 193–199.
37 Ricci, G.; Forni, A.; Boglia, A.; Motta, T.; Zannoni, G.; Canetti, M.; Bertini, F. Synthesis and X-ray structure of $CoCl_2(P^iPrPh_2)_2$. A new highly active and stereospecific catalyst for 1,2 polymerization of conjugated dienes when used in association with MAO. *Macromolecules* **2005**, *38*, 1064–1070.
38 Korthals, B.; Berkefeld, A.; Ahlmann, M.; Mecking, S. Catalytic polymerization of butadiene in aqueous systems with cationic nickel(II) complexes. *Macromolecules* **2008**, *41*, 8332–8338.
39 Bazzini, C.; Giarrusso, A.; Porri, L. Diethylbis(2,2′-bipyridine)iron/MAO. A very active and stereospecific catalyst for 1,3-diene polymerization. *Macromol. Rapid Commun.* **2002**, *23*, 922–927.
40 Gong, D.; Wang, B.; Cai, H.; Zhang, X.; Jiang, L. Synthesis, characterization and butadiene polymerization studies of cobalt(II) complexes bearing bisiminopyridine ligand. *J. Organomet. Chem.* **2011**, *696*, 1584–1590.
41 Jia, X.; Liu, H.; Hu, Y.; Dai, Q.; Bi, J.; Bai, C.; Zhang, X. Highly active and *cis*-1,4 selective polymerization of 1,3-butadiene catalyzed by cobalt(II) complexes bearing alpha-diimine ligands. *Chinese J. Catal.* **2013**, *34*, 1560–1569.
42 Alnajrani, M. N.; Mair, F. S. Synthesis and characterization of [small beta]-triketimine cobalt complexes and their behaviour in the polymerization of 1,3-butadiene. *Dalton Trans.* **2014**, *43*, 15727–15736.
43 Gong, D.; Wang, B.; Jia, X.; Zhang, X. The enhanced catalytic performance of cobalt catalysts towards butadiene polymerization by introducing a labile donor in a salen ligand. *Dalton Trans.* **2014**, *43*, 4169–4178.
44 Jie, S.; Ai, P.; Li, B. Highly active and stereospecific polymerization of 1,3-butadiene catalyzed by dinuclear cobalt(II) complexes bearing 3-aryliminomethyl-2-hydroxybenzaldehydes. *Dalton Trans.* **2011**, *40*, 10975–10982.
45 Liu, H.; Zhao, W.; Hao, X.; Redshaw, C.; Huang, W.; Sun, W. H. 2,6-Dibenzhydryl-*N*-(2-phenyliminoacenaphthylenylidene)-4-methylbenzenamine nickel dibromides: synthesis, characterization, and ethylene polymerization. *Organometallics* **2011**, *30*, 2418–2424.
46 Yu, J.; Hao, L.; Zhang, W.; Hao, X.; Sun, W. H. Access to highly active and thermally stable iron procatalysts using bulky 2-[1-(2,6-dibenzhydryl-4-methylphenylimino)ethyl]-6-[1-(arylimino)ethyl]pyridine ligands. *Chem. Commun.* **2011**, *47*, 3257–3259.
47 Sun, W. H.; Yang, H.; Li, Z.; Li, Y. Vinyl polymerization of norbornene with neutral salicylaldiminato nickel(II) complexes. *Organometallics* **2003**, *22*, 3678–3683.
48 Liu, H.; Zhuang, R.; Dong, B.; Wang, F.; Hu, Y. M.; Zhang, X. Q. Mono- andbinuclear cobalt(II) complexes supported by quinoline-2-imidate ligands: synthesis, characterization, and 1,3-butadiene polymerization. *Chinese J. Polym. Sci.* **2018**, *36*, 943–952.
49 Wang, B.; Gong, D.; Bi, J.; Dai, Q.; Zhang, C.; Hu, Y.; Zhang, X.; Jiang, L. Synthesis, characterization and 1,3-butadiene polymerization behaviors of cobalt complexes bearing 2-pyrazolyl-substituted 1,10-phenanthroline ligands. *Appl. Organomet. Chem.* **2013**, *27*, 245–252.
50 Nobbs, J. D.; Tomov, A. K.; Cariou, R.; Gibson, V. C.; White, A. J. P.; Britovsek, G. J. P. Thio-pybox and thio-phebox complexes of chromium, iron, cobalt and nickel and their application in ethylene and butadiene polymerisation catalysis. *Dalton Trans.* **2012**, *41*, 5949–5964.
51 Guo, J.; Wang, B.; Bi, J.; Zhang, C.; Zhang, H.; Bai, C.; Hu, Y.; Zhang, X. Synthesis, characterization and 1,3-butadiene polymerization studies of cobalt dichloride complexes bearing pyridine bisoxazoline ligands. *Polymer* **2015**, *59*, 124–132.
52 Gong, D.; Jia, X.; Wang, B.; Zhang, X.; Jiang, L. Synthesis, characterization, and butadiene polymerization of iron(III), iron(II) and cobalt(II) chlorides bearing 2,6-bis(2-benzimidazolyl)pyridyl or 2,6-bis(pyrazol)pyridine ligand. *J. Organomet. Chem.* **2012**, *702*, 10–18.
53 Cariou, R.; Chirinos, J. J.; Gibson, V. C.; Jacobsen, G.; Tomov, A. K.; Britovsek, G. J. P.; White, A. J. P. The effect of the central donor in bis(benzimidazole)-based cobalt catalysts for the selective *cis*-1,4-polymerisation of butadiene. *Dalton Trans.* **2010**, *39*, 9039–9045.
54 Chakraborty, B.; Banerjee, S. Synthesis, characterization, and crystal structures of cobalt(II), copper(II), and zinc(II) complexes of a bidentate iminophenol. *J. Coord. Chem.* **2013**, *66*, 3619–3628.
55 Van Wyk, J. L.; Mapolie, S. F.; Lennartson, A.; Håkansson, M.; Jagner, S. The catalytic oxidation of phenol in aqueous media using cobalt(II) complexes derived from *N*-(aryl) salicylaldimines. *Inorg. Chim. Acta* **2008**, *361*, 2094–2100.
56 Zhang, S.; Huang, Y.; Liu, X. Crystal and molecular structures of schiff base complexes with transition metal ions II. Bis-(*N*-(4-chlqro-phenyl)-salicylaldiminato)cobalt (II). *J. Struct. Chem.* **1991**, *10*, 242–244.
57 Lacroix, P. G.; Averseng, F.; Malfant, I.; Nakatani, K. Synthesis, crystal structures, and molecular hyperpolarizabilities of a new schiff base ligand, and its copper(II), nickel(II), and cobalt(II) metal complexes. *Inorg. Chim. Acta* **2004**, *357*, 3825–3835.
58 McKenzie, E. D.; Selvey, S. J.; Nowell, I. W. Stereochemistry of bissalicylaldiminatometal(II) compounds. Part III. Crystal and molecular structure of one form of bis-[*N*-(2,6-dimethylphenyl)salicylaldiminato] cobalt(II). *Inorg. Chim. Acta.* **1985**, *101*, 85–91.
59 Li, X.; Huang, L.; Dong, S.; Li, M.; Sun, H. Bis(3-*tert*-butyl-*N*,5-dimethylsalicylaldiminato)cobalt(II). *Acta Cryst.* **2005**, *E61*, 465–466.
60 Bahron, H.; Larkworthy, L. F.; Marécaux, A.; Povey, D. C.; Smith, G. W. Structures of bis(*N*-*n*-butylsalicylideneiminato)cobalt(II) and bis(*N*-*tert*-butylsalicylideneiminato)cobalt(II) complexes and reactivity towards oxygen and nitric oxide. *J. Chem. Cryst.* **1994**, *24*, 145–150.
61 Li, Z. X.; Zhang, X. L. Bis[4-chloro-2-(cyclohexyliminomethyl) phenolato]cobalt(II). *Acta Cryst.* **2005**, *E61*, 2806–2807.
62 Falivene, L.; Credendino, R.; Poater, A.; Petta, A.; Serra, L.; Oliva, R.; Scarano, V.; Cavallo, L. SambVca 2. A web tool for analyzing catalytic pockets with topographic steric maps. *Organometallics* **2016**, *35*, 2286–2293.

63 Falivene, L.; Cao, Z.; Petta, A.; Serra, L.; Poater, A.; Oliva, R.; Scarano, V.; Cavallo, L. Towards the online computer-aided design of catalytic pockets. *Nat. Chem.* **2019**, *11*, 872–879.
64 Falivene, L.; Cavallo, L.; Talarico, G. Buried volume analysis for propene polymerization catalysis promoted by group 4 metals: A tool for molecularmass prediction. *ACS Catal.* **2015**, *5*, 6815–6822.
65 Gao, Y.; Christianson, M. D.; Wang, Y.; Chen, J.; Marshall, S.; Klosin, J.; Lohr, T. L.; Marks, T. J. Unexpected precatalyst *σ*-ligand effects in phenoxyimine Zr-catalyzed ethylene/1-octene copolymerizations. *J. Am. Chem. Soc.* **2019**, *141*, 7822–7830.
66 Zhao, W.; Wang, B.; Dong, B.; Liu, H.; Hu, Y.; Eisen, M. S.; Zhang, X. 1-Hexene homopolymerization and copolymerization with polar *ω*-halo-*α*-alkenes by (benz)imidazolin-2-iminato scandium and yttrium complexes. *Organometallics* **2020**, *39*, 3983–3991.
67 Zhang, Y.; Wang, C.; Mecking, S.; Jian, Z. Ultrahighly branched main-chain-functionalized polyethylenes *via* inverted insertion selectivity. *Angew. Chem. Int. Ed.* **2020**, *59*, 14296–14302.
68 Dong, B.; Liu, H.; Peng, C.; Zhao, W.; Zheng, W.; Zhang, C.; Bi, J.; Hu, Y.; Zhang, X. Synthesis of stereoblock polybutadiene possessing *cis*-1,4 and syndiotactic-1,2 segments by iminopyridine cobalt complex-based catalyst through one-pot polymerization process. *Eur. Polym. J.* **2018**, *108*, 116–123.
69 Rhinehart, J. L.; Brown, L. A.; Long, B. K. A robust Ni(II) *α*-diimine catalyst for high temperature ethylene polymerization. *J. Am. Chem. Soc.* **2013**, *135*, 16316–16319.
70 Rhinehart, J. L.; Mitchell, N. E.; Long, B. K. Enhancing *α*-diimine catalysts for high-temperature ethylene polymerization. *ACS Catal.* **2014**, *4*, 2501–2504.
71 Wang, X.; Dong, B.; Yang, Q.; Liu, H.; Zhang, C.; Zhang, X. *α*-Diimine nickel complexes bearing axially bulky terphenyl and equatorially bulky dibenzobarrelene groups: synthesis, characterization and olefin polymerization studies. *Polym. Chem.* **2020**, *11*, 6783–6793.
72 Wang, X.; Dong, B.; Yang, Q.; Liu, H.; Hu, Y.; Zhang, X. Boosting the thermal stability of *α*-diimine palladium complexes in norbornene polymerization from construction of intraligand hydrogen bonding and simultaneous increasing axial/equatorial bulkiness. *Inorg. Chem.* **2021**, *60*, 2347–2361.
73 Ge, Y.; Li, S.; Wang, H.; Dai, S. Synthesis of branched polyethylene and ethylene-MA copolymers using unsymmetrical iminopyridyl nickel and palladium complexes. *Organometallics* **2021**, *40*, 3033–3041.

https://doi.org/10.1007/s10118-022-2758-5